Molecular Biology of the Cell
Vol. 20, 256–269, January 1, 2009

Alternative Requirements for Vestigial, Scalloped, and Dmef2 during Muscle Differentiation in *Drosophila melanogaster*

Hua Deng,*† Sarah C. Hughes,‡ John B. Bell,† and Andrew J. Simmonds*

*Department of Cell Biology, †Department of Biological Sciences, and ‡Department of Medical Genetics, University of Alberta, Edmonton, AB T6G 2H7, Canada

Submitted March 17, 2008; Revised October 14, 2008; Accepted October 29, 2008
Monitoring Editor: Marianne Bronner-Fraser

Vertebrate development requires the activity of the *myocyte enhancer factor 2* (*mef2*) gene family for muscle cell specification and subsequent differentiation. Additionally, several muscle-specific functions of MEF2 family proteins require binding additional cofactors including members of the Transcription Enhancing Factor-1 (TEF-1) and Vestigial-like protein families. In *Drosophila* there is a single *mef2* (*Dmef2*) gene as well single homologues of *TEF-1* and *vestigial-like*, *scalloped* (*sd*), and *vestigial* (*vg*), respectively. To clarify the role(s) of these factors, we examined the requirements for Vg and Sd during *Drosophila* muscle specification. We found that both are required for muscle differentiation as loss of *sd* or *vg* leads to a reproducible loss of a subset of either cardiac or somatic muscle cells in developing embryos. This muscle requirement for Sd or Vg is cell specific, as ubiquitous overexpression of either or both of these proteins in muscle cells has a deleterious effect on muscle differentiation. Finally, using both in vitro and in vivo binding assays, we determined that Sd, Vg, and Dmef2 can interact directly. Thus, the muscle-specific phenotypes we have associated with Vg or Sd may be a consequence of alternative binding of Vg and/or Sd to Dmef2 forming alternative protein complexes that modify Dmef2 activity.

INTRODUCTION

Specification and differentiation of both vertebrate and invertebrate muscles requires a conserved cohort of transcription factors (Baylies *et al.,* 1998; Cripps and Olson, 2002). Among these, myocyte enhancer factor-2 (MEF2) plays a key role in specification and subsequent differentiation of all muscle types (skeletal, smooth, and heart muscle; Lilly *et al.,* 1995; Black and Olson, 1998). There are four different known vertebrate *mef2* genes: *mef2-a*, *-b*, *-c,* and *-d* (Black and Olson, 1998). These four genes produce several different MEF2 isoforms involved in differentiation of all muscle types. In addition, it has been proposed that MEF2 proteins have a requirement for tissue-specific cofactors to confer additional specificity. For example, during mammalian heart development, GATA-4 (Charron and Nemer, 1999) helps to recruit MEF2 to the promoters of cardiac-specific genes including atrial natriuretic factor (ANF) and *α-cardiac actin* (*α-CA*; Morin *et al.,* 2000). MEF2 also interacts with another transcription factor, HAND1, during activation of ANF in cardiac cells (Morin *et al.,* 2005). This complex interplay between MEF2 proteins and cofactors is not restricted to cardiac muscles as during skeletal muscle development; MEF2 interacts with MyoD during activation of specific structural genes (Molkentin *et al.,* 1995; Black *et al.,* 1998).

In terms of MEF2 protein family activity, muscle differentiation in *Drosophila* is relatively less complex as there is only a single homologue *mef2*, *Dmef2* (Lilly *et al.,* 1994). Like vertebrates, *Drosophila* Dmef2 isoforms activate muscle-specific genes (Black *et al.,* 1998; Black and Olson, 1998) and also seems to interact with a conserved cohort of interacting proteins for muscle specification, including cardiogenesis. These include *tinman* (Azpiazu and Frasch, 1993), dHAND (Han *et al.,* 2006), and the gene encoding the GATA factor Pannier (Pnr; Gajewski *et al.,* 1997). Dissection of the regulatory region of the muscle-specific structural genes, *TroponinT* (Butler and Ordahl, 1999), *TroponinI* (*TnI*), and *Tropomyosin* (*TmI*) indicates that cofactors work together with Dmef2 during cardiogenesis in *Drosophila* (Lin *et al.,* 1996; Mas *et al.,* 2004; Nongthomba *et al.,* 2004). However, relatively little is known about the Dmef2 interacting partners during differentiation of somatic muscles (analogous to mammalian skeletal muscles) versus cardiac muscle cells. We have focused on the muscle-specific role of two proteins Scalloped (Sd) and Vestigial (Vg) that have been shown previously to be potent activators of fate specification in several nonmuscle cell types. There is considerable functional conservation in the activities of TEF-1/Sd and Vgl/Vg as mammalian TEF-1 can functionally substitute for Sd (Deshpande *et al.,* 1997) and Vgl-2 can partially substitute for Vg during *Drosophila* development (Vaudin *et al.,* 1999).

Sd is the only member of the Transcriptional Enhancer Factor-1 (TEF-1) family of proteins in *Drosophila* (Campbell *et al.,* 1992) and together with an activating cofactor, Vg, induce formation of the wing. In fact, ectopic expression of Vg, in the cells of the developing eye that also express Sd, leads to a respecification of these cells to a wing phenotype (Halder *et al.,* 1998; Simmonds *et al.,* 1998). Vg has two domains that influence transcriptional activation activity (MacKay *et al.,* 2003), and Vg requires Sd for nuclear localization (Halder *et al.,* 1998; Simmonds *et al.,* 1998; Srivastava

This article was published online ahead of print in *MBC in Press* (http://www.molbiolcell.org/cgi/doi/10.1091/mbc.E08–03–0288) on November 5, 2008.

Address correspondence to: Andrew J. Simmonds (andrew.simmonds@ualberta.ca).

et al., 2002). Both TEF-1 and Sd bind DNA via a conserved TEA domain, although like TEF-1, Sd does not exhibit significant transcriptional activation ability on its own. Vg interacts directly with Sd to form a transcription factor (TF) complex required for wing specific gene expression (Simmonds *et al.*, 1998). There is also evidence that TEF-1 acts in concert with other transcription factors. For example, YAP65 has been identified as a powerful transcriptional coactivator of TEF-1 in mouse (Vassilev *et al.*, 2001).

After identification of the Sd-interaction domain of Vg (Simmonds *et al.*, 1998), several mammalian genes encoding Vestigial-like proteins with homologous domains were identified. These include Vestigial-like 2 (Maeda *et al.*, 2002a), which interacts with TEF-1 in skeletal muscle to augment myosin heavy chain (MHC) expression (Maeda *et al.*, 2002a; Gunther *et al.*, 2004). Vestigial-like 4, which is enriched in heart muscle also functionally interacts with TEF-1 (Chen *et al.*, 2004). Similarly, the Sd homologue, TEF-1 is an MEF2-interacting protein expressed in all muscle types (Stewart *et al.*, 1994; Carlini *et al.*, 2002). The phenotype of a TEF-1 mouse knockout suggests a role in cardiac maturation (Chen *et al.*, 1994), but TEF-1 is also required for skeletal and smooth muscle gene expression (Pasquet *et al.*, 2006). However, TEF-1 cannot activate transcription alone (Xiao *et al.*, 1991), and overexpression of TEF-1 results in repression of transcription (Jiang and Eberhardt, 1996).

In terms of muscle development, mammalian TEF-1 has been shown to interact with MEF2, and this interaction interferes with MEF2-dependent activation of the β-Myocyte heavy chain (β-MHC) promoter (Maeda *et al.*, 2002b). Other known MEF2 cofactors include poly-(ADP-ribose) polymerase (PARP) on the cardiac TnT gene (Butler and Ordahl, 1999), Max on the cardiac α-myosin heavy-chain gene (Gupta *et al.*, 1997), and serum response factor on the skeletal α-actin gene (Gupta *et al.*, 2001). Given the multiplicity of interactions between these proteins, it is possible that MEF2 and TEF-1 function within a larger complex of TFs that includes additional proteins, like members of the Vgl family and that alternative composition of these various complexes may provide cell-specific gene activation during muscle differentiation.

Although Dmef2 has a clear role in *Drosophila* muscle differentiation, specific functions for Vg or Sd in muscle cells has not yet been well characterized. To test the role for a complex of MEF2, TEF-1, and the Vgl-family of proteins in the differentiation of muscle cells led us to probe the combinatorial activities of each of these proteins during *Drosophila* embryonic muscle specification. There is some precedence for a role for Vg in muscle development as it had been reported to be required for late-stage development of indirect flight muscles (IFMs) derived from the wing disk–associated myoblasts (Sudarsan *et al.*, 2001). In wing discs isolated from flies with null *vg* mutations, myoblasts proliferate, migrate, and fuse normally but further differentiation fails to occur (Bernard *et al.*, 2003), a phenotype similar to that associated with mutations in *Dmef2* (Nguyen and Xu, 1998; Nguyen *et al.*, 2002). Although it is possible that this phenotype is due to the well known wing-specification role previously ascribed to Vg, it is equally possible that this represents a muscle-specific activity for Vg and Dmef2 and further suggests that these two proteins may functionally interact.

To clarify the role of Sd and Vg during embryonic muscle development, in addition to the IFM precursors, we have looked at all of the developing muscles in *sd* and *vg Drosophila* mutant embryos and found consistent defects in both the cardiac and somatic musculature. Additionally, we have shown that *sd* is expressed in at least some *Drosophila* embryonic muscles. Further, we have tested protein interactions between *Drosophila* Dmef2, Sd, and Vg and found that these proteins do interact both in vitro and in vivo. Finally, we have tested the specific combinatorial requirement for the presence or absence of Vg or Sd in certain muscle types because elevated expression of each causes significant defects in the specification or differentiation of specific muscle cell types.

MATERIALS AND METHODS

Cell Culture and Transfections

Drosophila S2 cells were grown at 25°C in Schneider's *Drosophila* medium (Invitrogen, Carlsbad, CA) supplemented with 10% fetal bovine serum. Transfections were carried out using dimethyldioctadecyl-ammonium (Han, 1996).

Drosophila Strains

Ectopic-expression of Gal4-UAS transgenes (Brand and Perrimon, 1993) was performed using Dmef2-Gal4 (Ranganayakulu *et al.*, 1998), Sd-Gal4 (Roy *et al.*, 1997), and *5053*-Gal4 (Ritzenthaler *et al.*, 2000). All other UAS-transgene animals were made in our laboratory for this study.

Plasmids

GST-Sd and GST-Dmef2 vectors were created by insertion of full-length *sd* and *Dmef2* into the BamHI and SalI sites of pGEX-4T1 (GE Biotech, Piscataway, NJ), respectively. Vg deletions (see Figure 5) in pET16b (Novagen, Madison, WI) were as described previously (Simmonds *et al.*, 1998). Expression vectors for transfection of S2 cells (see Figure 4) were created by Gateway Technology (Invitrogen) and the *Drosophila* Gateway destination vectors (Terrence Murphy, Carnegie Institute of Washington, Baltimore, MD).

Fluorescent In Situ Hybridization

Anti-sense digoxigenin (DIG, Roche, Indianapolis, IN) RNA probes targeting *sd* were made by creating a double-stranded PCR product with a T7 polymerase binding site incorporated into the 3′ primer. The primers used were 5′-gaacaacctgagctgcagcgagttgg and 5′-taatacgactcactatagggagacagcacttggatgtgcg. Embryo fixation and hybridization of the probes and detection of the fluorescent signal were performed using the method of Hughes and Krause (1999), including the modifications outlined in Lecuyer *et al.* (2007).

Glutathione S-Transferase Pulldown Assays

Glutathione *S*-transferase (GST) fusion proteins were expressed in *Escherichia coli* [Rosetta 2(DE3), Novagen] and purified according to the manufacturer's directions (GE Biotech). Probe proteins were ^{35}S labeled in vitro using the TNT-coupled in vitro transcription-translation system (Promega, Madison, WI). For the in vitro binding assay, 3–6 μl of ^{35}S-labeled probe proteins were incubated with 2 μg of immobilized GST fusion proteins in 500 μl of buffer (20 mM Tris, pH 7.6, 100 mM NaCl, 0.5 mM EDTA, 10% glycerol, and 1% Tween-20) containing 0.25% bovine serum albumin (BSA) and protease inhibitor cocktail for 2 h at 4°C. The beads were washed six times in 500 μl of the same buffer, and the bound proteins were resolved by SdS-PAGE and analyzed by autoradiography.

Immunoprecipitations and Immunoblotting

S2 cells were transfected with relevant expression constructs containing the heat-shock promoter, and protein expression was induced by heat shocking cells for 35 min at 37°C. Cells were harvested 1 h after induction, washed one time in PBS, and resuspended in RIPA (radio-IP) buffer (50 mM Tris, pH 8.0, 150 mM NaCl, 1.0% NP-40, 0.5% deoxycholic acid, 0.1% SdS, and protease inhibitor cocktail). The lysate was then incubated for 15 min at 4°C with agitation and centrifuged for 15 min at 13.2K rpm at 4°C, and the supernatant was then transferred to a fresh tube. CoIP reactions were carried out on 200 μl of supernatant (600 μl supernatant from a 25-cm^2 flask of cell culture) using 8 μl anti-FLAG M2-agarose (Sigma, St. Louis, MO) in 500 μl RIPA buffer. Agarose beads were incubated for 1 h at 4°C with rocking, centrifuged for 1 min at 1.4K rpm at 4°C, and washed six times by vortexing in 500 μl RIPA buffer. Primary antibodies for immunoblotting were mouse anti-FLAG (1:1000; Sigma), rat anti-hemagglutinin (HA; 1:400; Roche), and rabbit anti-Myc (1:1000; Cell Signaling, Beverly, MA). Secondary antibodies were goat anti-mouse Alexa680 or IRdye800 (1:5000; Invitrogen), goat anti-rabbit Alexa 680 or IRdye800 (1:5000; Invitrogen), and goat anti-rat IRdye800 (1:5000; Invitrogen). Nitrocellulose membranes were scanned and analyzed by Odyssey Infrared Imaging System (Li-Cor Biosciences, Lincoln, NE).

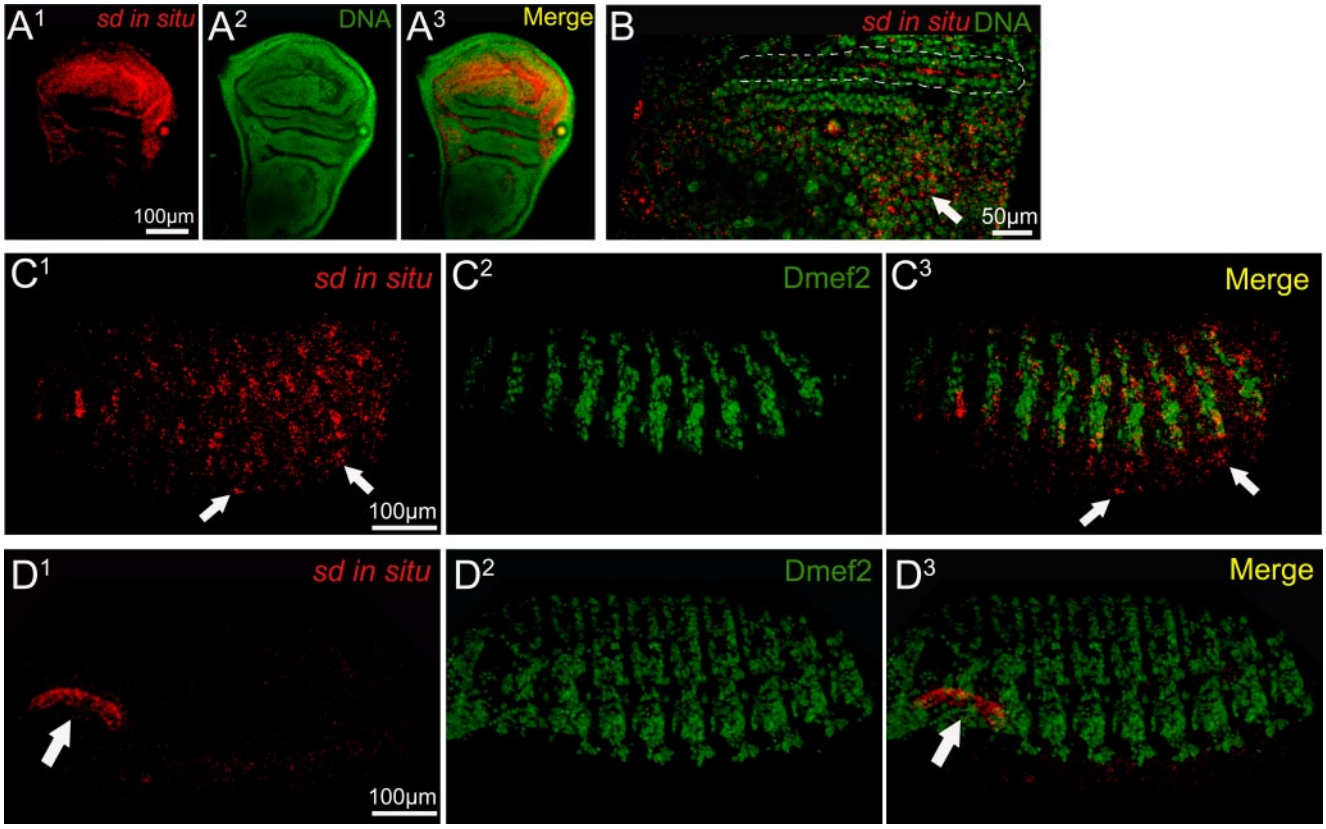

Figure 1. *sd* in situ reveals the expression of *sd* in both SMs and dorsal vessel. (A^1–A^3) The specificity of the *sd* probe for in situ was tested on wing disk, and *sd* expression pattern in wing disk was accurately revealed by this probe. (B) *sd* transcript was found mostly in the heart region of the dorsal vessel (dashed line). It also appears in the hind gut (arrow). (C^1–C^3) *sd* transcript was detected in SMs of stage 13 wild-type embryos. SMs are visualized by Dmef2 staining. *sd* transcript was also detected in the CNS cells (arrows). (D^1–D^3) It failed to detect *sd* transcript in SMs of wild-type embryos at early stage 16. High expression of *sd* was found in salivary gland at this stage (arrow).

Reverse Transcriptase PCR

Total RNA from stage 12–15 wild-type embryos and overexpression embryos was isolated with Trizol reagent (Invitrogen) and treated with *DNase I* (Ambion, Austin, TX). Reverse transcription was carried out using 2 μg of total RNA, SuperScript II reverse transcriptase (SS II, Invitrogen) and gene-specific first-strand primers. Subsequent amplification of the resulting cDNA was performed using *Taq* DNA polymerase (Invitrogen) and one pair of nested primers for each gene. Primers for the control *rp49* cDNA were: first-strand primer, 5′-cttcttgagacgcaggcga and nested primers, 5′-agcatacaggcccaagatcg and 5′-agtaaacgcgggttctgcat. Primers for *Act57B* cDNA amplification were first-strand primer, 5′-gcaggagacaggtgagtagacc and nested primers, 5′-ctccggcatgtgcaagg and 5′-gcaacacgcagctcgttg. Primers for *mhc* cDNA amplification were 5′-agaaggctgaggaactgc and 5′-gttcaagttgcggatctg. The primers were designed for *rp49* and *mhc* to span an intron and the forward primer for *Act57B* cDNA to span the conjunction of two exons. To make sure the RT-PCR was in the linear range of amplification, we performed PCR reactions at increasing cycle numbers (15, 20, 25, and 30), and similar results were observed. The RT-PCR was performed on two different mRNA isolations, and repeated three times, with consistent results.

Fluorescence Microscopy

Wild-type and overexpression embryos were fixed and stained with various antibodies as described previously (Hughes and Krause, 1999). The following primary antibodies were used at the indicated concentrations: mouse anti-FLAG (1:1000; Sigma); rat anti-HA (1:200; Roche); rat anti-Myosin (1:500; Abcam, Cambridge, MA); mouse anti-Myc (1:300; Cell Signaling); rabbit anti-Dmef2 (1:1000; from B. Paterson, National Cancer Institute, Bethesda, MD); rabbit anti-Tinman (1:1000); mouse anti-βPS-integrin (developed by Danny Brower and obtained from the Developmental Studies Hybridoma Bank, The University of Iowa, Department of Biological Sciences, Iowa City, IA, 1:500); mouse anti-β-Gal (Promega, 1:500). Alexa488-, Alexa568-, Alexa594-, and Alexa647-conjugatged secondary antibodies (Invitrogen) were used to recognize the primary antibodies. Muscle actin was stained by Alexa546-conjugated phalloidin (Invitrogen, 1:25). Images were obtained using a spinning disk confocal system (Ultraview ERS; Perkin Elmer, Norwalk, CT) mated to a CS9100-50; camera (Hamamatsu, Bridgewater, NJ), and an Axiovert 200M microscope (Carl Zeiss MicroImaging, Thornwood, NY) using Ultraview ERS software (Version 2, Perkin Elmer) and assembled with Adobe Photoshop (Ver. CS, San Jose, CA; using Windows XP, Microsoft, Redmond, WA).

RESULTS

Sd Is Expressed in a Subset of Developing Somatic and Cardiac Muscle Cells

We used two independent methods to examine various aspects of *sd* expression in *Drosophila* embryos. We first performed fluorescent in situ hybridization (FISH) to detect *sd* mRNA. Although it appears that *sd* mRNA is expressed at low levels in most cells in developing embryos requiring extensive signal intensification, the specificity of our *sd* probe was verified by examining wing imaginal discs where elevated levels of *sd* mRNA are seen in the dorsal-ventral region (Figure 1A). In developing embryos, elevated levels of *sd* mRNA were found mostly in the heart region of the dorsal vessel and in SMs of stage13 wild-type embryos (Figure 1, B and C), although we could no longer detect elevated Sd transcript levels in SMs of wild-type embryos at early stage 16 compared with the staining observed in other tissues (i.e., salivary glands, Figure 1D).

We also tested the muscle-specific expression of two different well-characterized reporter constructs that express *β-galactosidase* (*β-gal*) under the control of *sd* enhancers. sd^{ETX4} animals have an enhancer-trap (*β-gal*) P-element construct inserted into the 5′ regulatory region of the *sd* locus

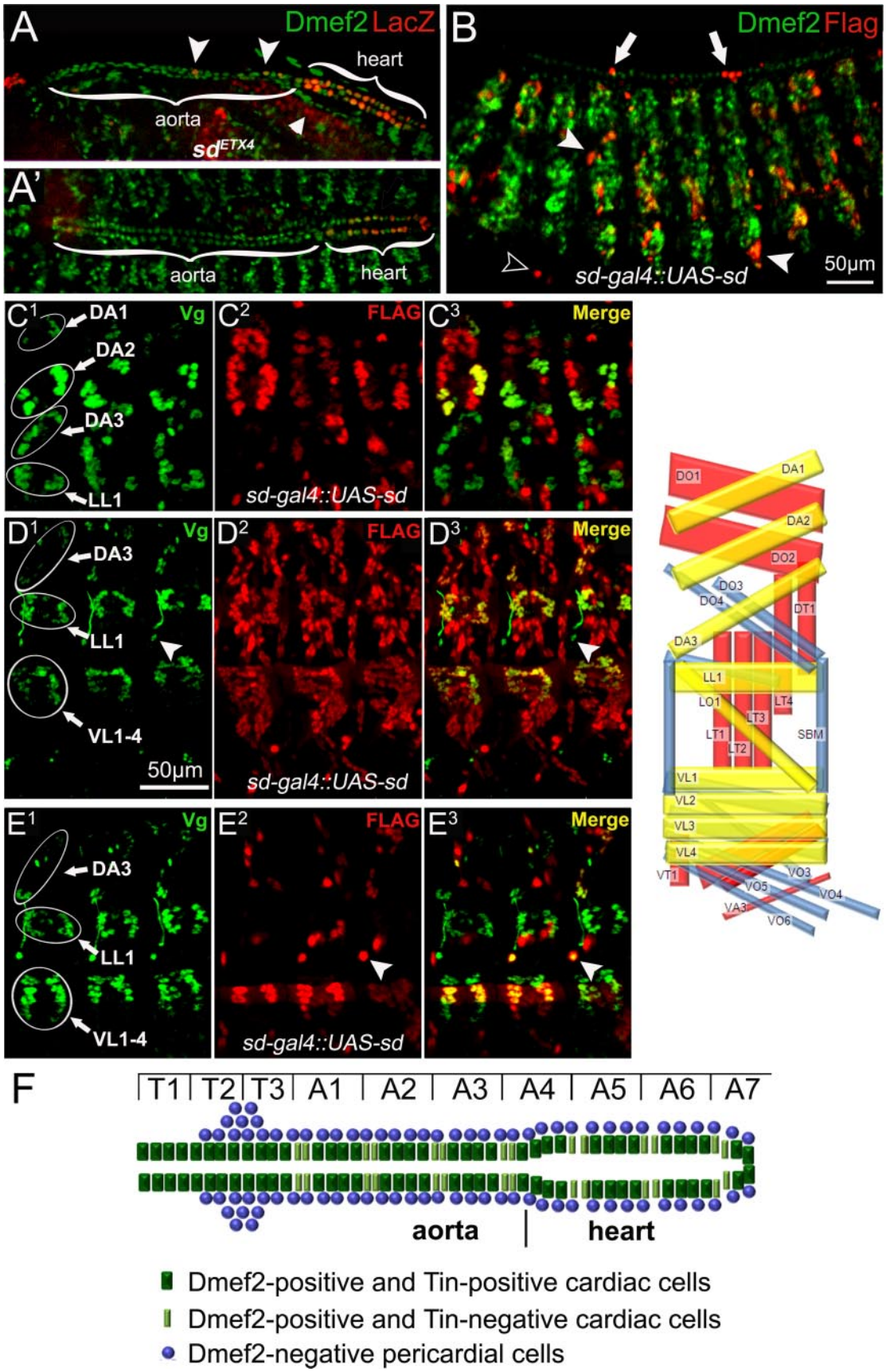

Figure 2. *sd*, *vg*, and *Dmef2* are coexpressed in embryonic muscles. To facilitate double staining, *sd* expression was detected by examining *sd* reporter constructs ($sd^{ETX4,}$ A and A'), or using 3xFLAG-Sd driven by *sd*-GAL4 (B–E). Muscle cells are marked with anti-Dmef2 (green

and have been used extensively to obtain the pattern of *sd* expression in embryo and other tissues (Campbell *et al.*, 1992; Deshpande *et al.*, 1997; Varadarajan and VijayRaghavan, 1999; Muller *et al.*, 2005). Similar to what we observe with FISH detection of the *sd* signal, in sd^{ETX4} embryos, significant levels of *β-gal* can be detected in some muscle cells (Figure 2A). This includes cardiac cells at stage 13 (data not shown), and by stage 16 *β-gal* is expressed in almost all cardiac cells in the heart region of the dorsal vessel (Figure 2A).

We also tested a second *sd*-GAL4 enhancer trap reporter line with the P-element inserted into the first intron of the *sd* locus, which matches the wing-specific expression of sd^{ETX4} (Roy *et al.*, 1997). An advantage to this GAL4 based reporter is that we could use it to induce expression of a UAS-*3xFLAG*-Sd transgene. This allows the examination of a FLAG-tagged Sd under the control of an endogenous *sd* enhancer, closely mirroring the cellular produrance of the endogenous Sd protein. This consideration is important as *sd* expression driven by *sd*-GAL4 appears to be very dynamic. At stage 13, it drives expression in 31% cells of SMs and several cardiac cells (Figure 2, B and C). At early stage 16, it drives expression in all SMs but not in heart cells (Figure 2D). The expression appears to drop during late stage 16 and is restricted to only some ventral SMs (Figure 2E). It appears that *sd*-GAL4 induced expression of *3xFLAG-sd* does not cause any dominant-negative changes to the somatic or cardiac muscle specification in embryos (Figure 2, B–F). We also analyzed the expression of UAS-*β-gal* driven by *sd*-GAL4. The *β*-Gal protein is extremely stable, which although makes interpretation of the dynamic nature of *sd*-GAL4 expression difficult in earlier stages, allowed us to confirm that expression is restricted to ventral SMs, the same as that of *3xFLAG-sd* at late stage 16 (data not shown).

vg Is Expressed in Embryonic SMs But Not Heart Muscle

We used an anti-Vg antibody to correlate *vg* expression with that of the *sd*-reporters in embryonic muscles (Figure 2, C–E). *3xFLAG*-Sd expression does not affect the expression of *vg* in muscle cells, because *vg* has the same expression pattern as in wild type. Vg is first detected at stage 11 in the progenitors of ventral SMs, VL1-4 (data not shown; see Figure 2 for the diagram of each muscle identity). Then it is present in the muscles, LL1 and DA1-3, at stage 13 (Figure 2C). Vg is also present in VL1-4, LL1, and DA1-3 when 3xFLAG-Sd appears in all SMs of early stage 16 embryos (Figure 2D) and when the expression of *3xFLAG*-Sd fades and is restricted to some ventral SMs at late stage 16 (Figure 2E). After late stage 17, Vg cannot be reliably detected in muscle cells, confirming what has been reported previously (Baylies *et al.*, 1998).

Both the sd^{3L} and vg^{null} Mutations Cause Defects in Embryonic Muscle Development

The X-linked, recessive, sd^{3L} allele is homozygous lethal. Sequencing of sd^{3L} identified a T-A substitution producing a premature stop codon (Srivastava *et al.*, 2004). The sd^{3L} likely represents a strong loss-of-protein-function allele because some hemizygous male animals do hatch and survive as feeble larvae with behavioral abnormalities that maybe result from muscle defects (Campbell *et al.*, 1991). For example, recently hatched wild-type larvae have characteristic contraction waves that pass from the posterior to anterior and are responsible for locomotion. We found that the waves of contraction are much slower in sd^{3L} hemizygotes, taking approximately three times as long to pass from posterior tip to anterior tip compared with wild type. Notably, examination of the embryonic muscles of sd^{3L} hemizygotes revealed defects in both heart and somatic muscle development (Figure 3, A–G). Many of these embryos (30%) have less than the wild-type number of cardiac cells (Figure 3C), and many of the remaining cardiac cells have nuclei larger than normal (Figure 3, A and B). In many of the mutant embryos we also see somatic muscle defects, most often the ventral SMs (VO4-6) get lost or have defects in development (Figure 3, D and E). Actin staining also revealed that the VO4-6 muscles disappeared in some segments (Figure 3, F and G).

The vg^{null} mutant is homozygous viable but with severely reduced viability compared with wild-type flies including female sterility (Bernard *et al.*, 2003). vg^{null} larvae showed similar muscle contraction defects to those associated with sd^{3L}, taking approximately two times as long for the contraction waves to reach the anterior tip compared with wild type. Actin staining showed that the VL2 muscle was often missing in vg^{null} embryos (Figure 3, F and H) with no detectable defects in other muscles. This phenotype is enhanced in *Dmef2* RNA interference (RNAi) background (Supplemental Figure 2F), indicating a functional interaction between these two genes.

Sd, Vg, and Dmef2 Can Form a Multiprotein Complex

As some interaction of the mammalian homologues of Sd, Vg, and Dmef2 has been reported previously, coimmunoprecipitation (coIP) was performed from S2 cell lysates expressing epitope-tagged Vg, Sd, or Dmef2. These three proteins appear to form a tripartite complex as any two could be coIPed with the third (Figure 4A). For example, coIPs of 3xFLAG-Sd also could detect 3xHA-Vg and 6xMyc-Dmef2 (Figure 4A). Similar results were observed when we used 3xFLAG-Vg or 3xFLAG-Dmef2 to coIP the other two proteins (data not shown). The interactions between any two of these three proteins appear to be independent of the third, as coIP of any two does not require the coexpression of the third (Figure 4, B and D). To further test for the possibility that Vg is required for the interaction between Sd and

Figure 2 (cont). in A and B), and Vg is labeled by anti-Vg (green in C–E). 3xFLAG-Sd and LacZ are visualized with anti-FLAG and anti-*β*-Gal (red), respectively. (A) In stage 16 embryos the sd^{ETX4} reporter is activated in the heart region of the dorsal vessel and in some cardiac cells in the aorta region (arrowheads). It is also expressed in the hind gut, underneath the visceral muscles (VMs, small arrowhead). (A) A dorsal-lateral view; (A′) a dorsal view. (B) *sd*-GAL4 drives expression of 3xFLAG-Sd in several cardiac cells (arrows) and ~31% cells of somatic muscles (SMs, arrowheads) at stage 13. Note that *sd*-GAL4 is also activated in cells of central neuron system (CNS, empty arrow). Dmef2 is present in all muscle cells. C^1–C^3 shows the dorsal SMs where *vg* is expressed at stage 13. 3xFLAG-Sd can be detected in some SMs. D^1–D^3 shows that *vg* is expressed in the DA3, LL1, and VL1-4 muscles when 3xFLAG-Sd appears in all SMs at stage 16. Vg also appears in some neuronal cells (arrowheads). DA1-2 are not shown because they are out of the field of view. E^1–E^3 shows that *vg* is still expressed in the DA3, LL1, and VL1-4 muscles when the expression of 3xFLAG-Sd fades in SMs and appears only in some ventral SMs at late stage 16. At this stage, 3xFLAG-Sd appears with Vg in the neuron cells shown above (arrowheads). (F) A schematic drawing of a stage 16 embryonic dorsal vessel (dorsal view, anterior to the left). Heart cells include two parallel rows of Dmef2-positive cardiac cells in the middle with four Tinman-positive cardiac cells per hemisegment starting from T1. Dmef2-negative pericardial cells surround the cardiac cells. On the right is a schematic representation of the embryonic SMs in each abdominal hemisegment A2–A7 (lateral view with anterior up) using the nomenclature of Crossley (1978). Inner, middle, and outer muscle layers are shown in yellow, blue, and red, respectively (Bate and Rushton, 1993).

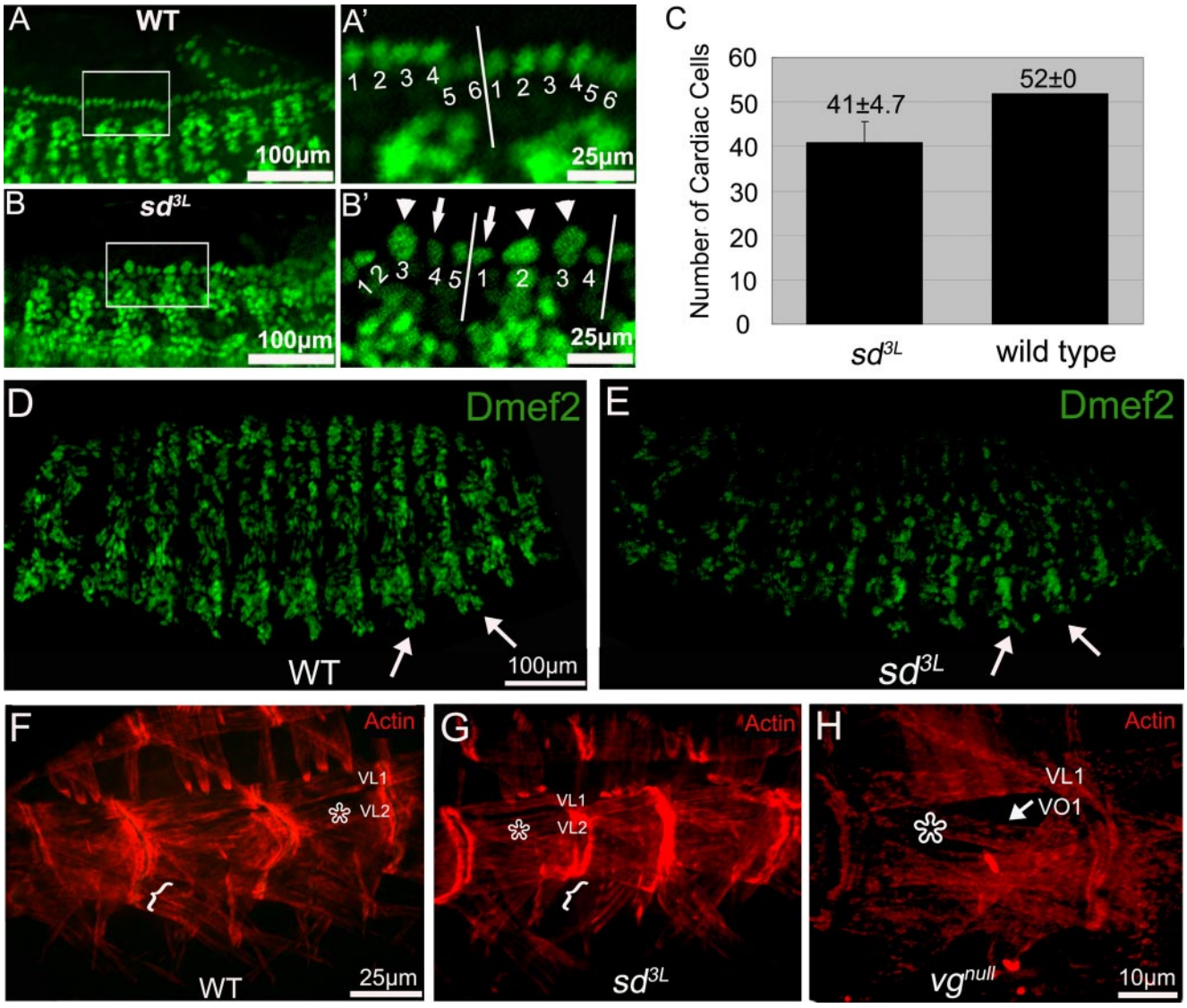

Figure 3. The sd^{3L} and vg^{null} mutants have defects in embryonic muscle development. Muscle cells are marked with anti-Dmef2 (green), and muscle fibers are visualized by phalloidin staining (red). Anterior is to the left. (A) In stage 13 wild-type embryos (A′ is the close-up of the boxed area in A), there are six cardiac cells per hemisegment (A′). (B) In stage 13 sd^{3L}mutant embryos (B′ is the close-up of boxed area in B), there are many cardiac cells with enlarged nuclei (arrowheads) relative to neighboring cells (arrows), and there are fewer cardiac cells per hemisegment (compare A′ with B′). (C) The number of cardiac cells on one side of sd^{3L} embryos (41 ± 4.7, mean ± Sd, n = 8) is less than that of wild type (52 ± 0, n = 10). (D) The SMs of a wild-type embryo at early stage 16. (E) The SMs of a sd^{3L}mutant embryo at the same stage. Many ventral SMs (VO4-6, see Figure 2) have severe developmental defects or are absent entirely (arrows, compare E with D). (F) Actin was stained by phalloidin in a stage 16 wild-type embryo. The VO4-6 muscles are indicated by a bracket and the VL2 muscle is demarked by an asterisk. (G) In the sd^{3L} mutant, the VO4-6 muscles is absent in some segments (bracket). (H) In the vg^{null} mutant, the VL2 muscle is absent in some segments (star), and the VO1 muscle underneath can be seen (arrow).

Dmef2, sequential IPs were performed by first isolating 3xFLAG-Sd and 6xMyc-Dmef2 or 3xFLAG-Dmef2 and 6xMyc-Sd and then testing for the presence of Vg. In either case, Vg was not detected (Figure 4C). Time-course IPs were also performed to test the specificity of the interaction between Vg and Dmef2 (Figure 4D). This interaction appears to be highly specific, because the amount of 6xMyc-Dmef2 IPed by 3xFLAG-Vg increases with time.

Vg Interacts with Dmef2 and Sd at Different Sites

Because Vg, Sd, and Dmef2 interact, it is possible that they bind alternatively to the same sites or simultaneously at different locations. To map the region within Vg that interacts with Dmef2, GST pulldown assays (Kaelin *et al.*, 1991) were performed. We first confirmed that Vg can bind directly with Dmef2 (Figure 5A). We then tested deleted or truncated forms of Vg and found that only one Vg deletion, Vg3-9, did not interact with Dmef2 (Figure 5, B–D). This indicates that at least two independent domains within Vg participating in binding to Dmef2: one within amino acids 1-187 and the other within amino acids 279-336 (Figure 5C). The Sd-interaction domain of Vg has been mapped to amino acids 279–336 (Simmonds *et al.*, 1998). We note that there is some residual binding of one of the deletions (Vg 1-4) with the GST control. However, the much stronger signal obtained when GST-Dmef2 is present makes us confident that

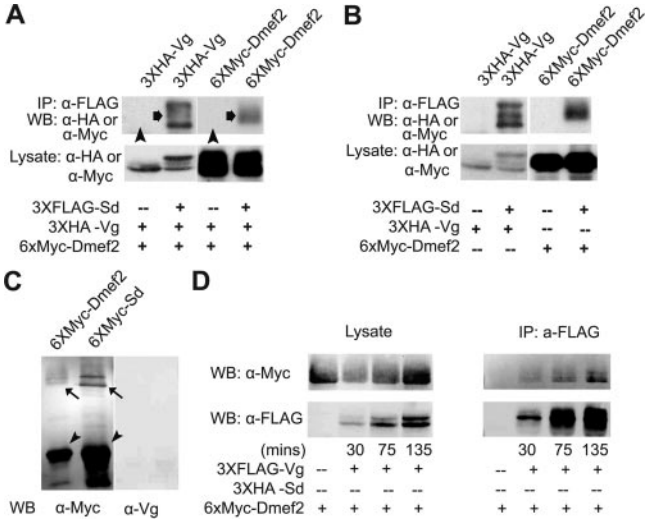

Figure 4. Interactions between Sd, Vg, and Dmef2 can be shown by coimmunoprecipitation (CoIP) assays. Indicated proteins with different tags were coexpressed in S2 cells, and CoIP was performed using anti-FLAG beads in both control and experiment samples. Proteins coming down with the beads and the relative expression level of the proteins in the lysate were detected with corresponding tag antibodies. (A) Dmef2 and Vg were coIPed simultaneously with Sd (arrows). In the control, tagged Vg and Demf2 did not come down with the beads (arrowheads). There are additional bands for Vg and Dmef2, likely because of posttranslational modifications. (B) Sd coIPed Vg or Dmef2 without coexpression of Dmef2 or Vg, respectively. (C) The anti-FLAG bead-purified IP complex of 3xFLAG-Sd and 6xMyc-Dmef2 and that of 3xFLAG-Dmef2 and 6xMyc-Sd were immunoblotted with anti-Myc and anti-Vg antibodies. Significant levels of Vg could not be detected in these complexes. Arrows show the proteins coming down with the beads, and arrowheads show the primary antibody bands. (D) CoIP was performed on S2 cells transfected with the indicated proteins at different times, following heat shock. The relative amount of coIPed Dmef2 (right) increased with the expression level of Vg and Dmef2 (left).

this residual binding is due to weak, nonspecific "stickyness" of the N-terminal region of Vg. Because Vg8-9, a deletion that removes the Sd interacting region, still interacts strongly with Dmef2 (Figure 5B), Vg could potentially interact with Sd and Demf2 at the same time via different domains.

Altering Vg and/or Sd Levels Affects the Expression of Known Muscle Differentiation Genes

To test the functional consequence of altering the relative levels of Vg and/or Sd in a complex with Dmef2, we next tested the functional consequence of altering the levels of Vg or Sd in various differentiating muscle types. Dmef2 is highly expressed in the developing midgut (Figure 6A). Elevated expression of Vg (Figure 6B) in these tissues does not have any obvious effect on muscle differentiation. However, elevating the expression of Vg and Sd together or Sd alone causes the loss of tissue-specific constrictions (Figure 6C). This overexpression does not affect the expression level of Dmef2 (Figure 6C) and cause a phenotype similar to a *Dmef2* deletion mutant (Lilly *et al.*, 1995). In the somatic muscles, expression of a known Dmef2 target, myosin is affected when Sd is present, and this effect is enhanced when both Vg and Sd are present (Figure 6, D–F). This phenotype is similar to that of embryos overexpressing a Dmef2 inhibitor, Him in SMs (Liotta *et al.*, 2007). We observed a similar reduction in actin staining when Vg and Sd were overexpressed in cells also expressing Dmef2 (Figure 6, G–H). We then tested the mRNA levels of two known Dmef2 target genes, *actin57B* (*act57B*) and *myosin heavy chain* (*mhc*). *Drosophila* Act57B is the major myofibrillar actin expressed in skeletal, visceral, and cardiac muscle during embryogenesis, and there is a conserved Dmef2-binding site within the promoter that is necessary for the full expression of *act57B* in embryos (Kelly *et al.*, 2002). Similarly, *mhc* expression is significantly reduced in *Dmef2* mutants (Lilly *et al.*, 1995). When elevated levels of Sd and Vg are present in *Dmef2*-

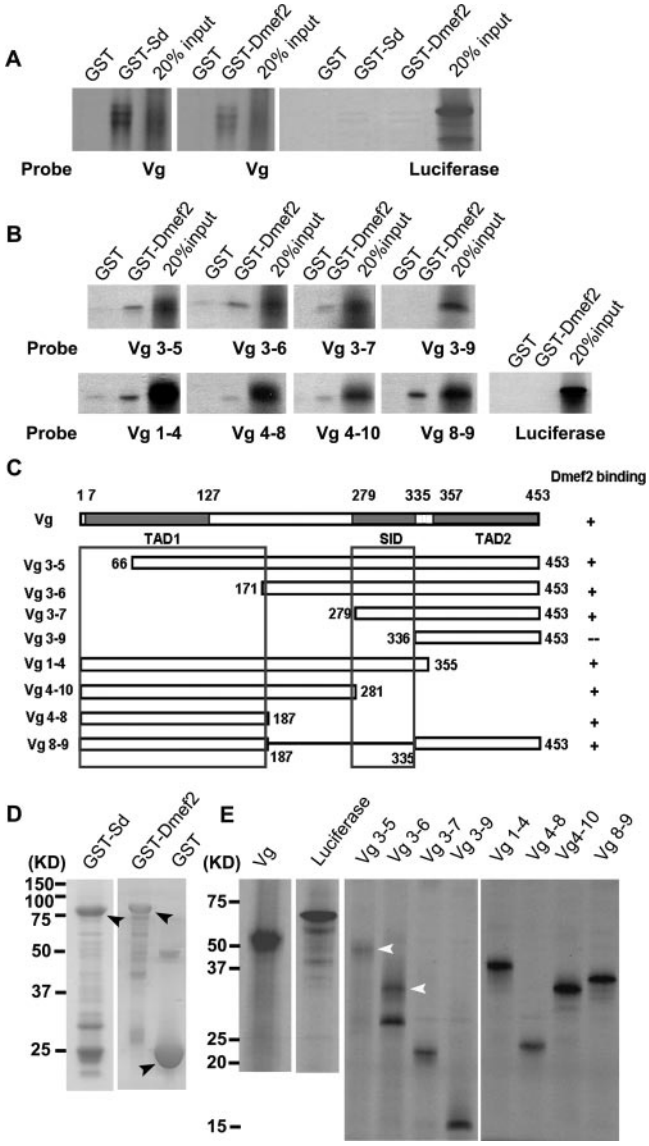

Figure 5. Vg can interact with Dmef2 at a different site than it interacts with Sd. (A) A positive control shows an interaction with a known Vg binding partner (GST-Sd). A similar robust interaction is detected between Vg and GST-Dmef2. Luciferase serves as a negative control. (B) Two separate domains (illustrated with boxes in C) in Vg are capable of interacting with Dmef2. All deletions except Vg3-9 interact with GST-Dmef2 because at least one of the two domains is intact in all other deletions tested. (D and E) Gel analysis confirming expression of proteins used in pulldown assays (arrowheads). Protein size is indicated on the left. SID, Sd interaction domain; TAD, transcription activation domain.

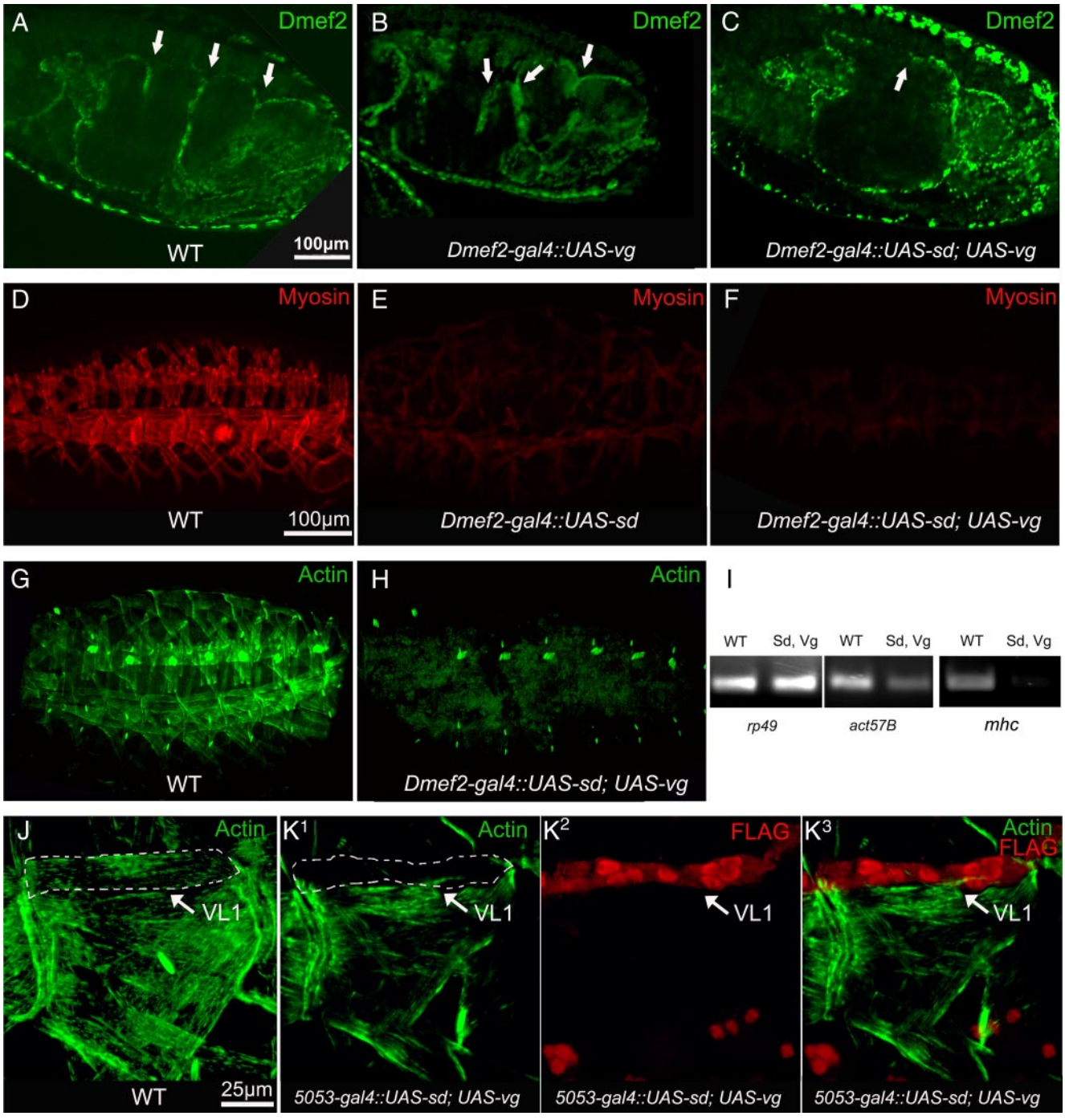

Figure 6. The Sd–Vg complex represses Dmef2 function during muscle differentiation. Embryos (stage 16) are shown as lateral views, and dorsal is up, with anterior to the left. (A) The three constrictions that subdivide the midgut into four chambers are shown with arrows in a wild-type embryo. (B) Ectopic expression of Vg in visceral muscles of embryos via *Dmef2*-GAL4 does not affect the formation of these constrictions. (C) Ectopic coexpression of Sd and Vg in visceral muscles leads to the repression of Dmef2 function in these muscles and all three constrictions disappear. (D–F) The Myosin staining of wild-type embryos (D) and the embryos overexpressing Sd or Sd and Vg (E and F). The apparent level of myosin staining is reduced when Sd is overexpressed in *Dmef2*-expressing muscles (E) and even more reduced when Vg and Sd are present (F). (G and H) Actin staining by phalloidin failed to show the formation of myofibers in muscles of embryo overexpressing Sd and Vg. (I) The results of RT-PCR from stage 12–15 wild-type embryos or embryos overexpressing Sd and Vg. The relative amount of *act57B* and *mhc* mRNA in embryos overexpressing Sd and Vg is much lower than wild type. *rp49* mRNA was used as loading control. (J) Ventral SMs in one segment are visualized by actin staining in a wild-type embryo, and VL1 is shown by the dashed frame. (K^1–K^3) Specific overexpression of Sd and Vg in VL1 via *5053*-GAL4 leads to the missing of myofiber in this muscle. (Sd and Vg are 3xFLAG tagged and 3xHA tagged, respectively).

expressing cells, a significant reduction in both *act57B* and *mhc* mRNA are observed (Figure 6I). To confirm that the effect we see on suppression of actin or myosin is specific to the presence of Vg and Sd, we also expressed these trans-

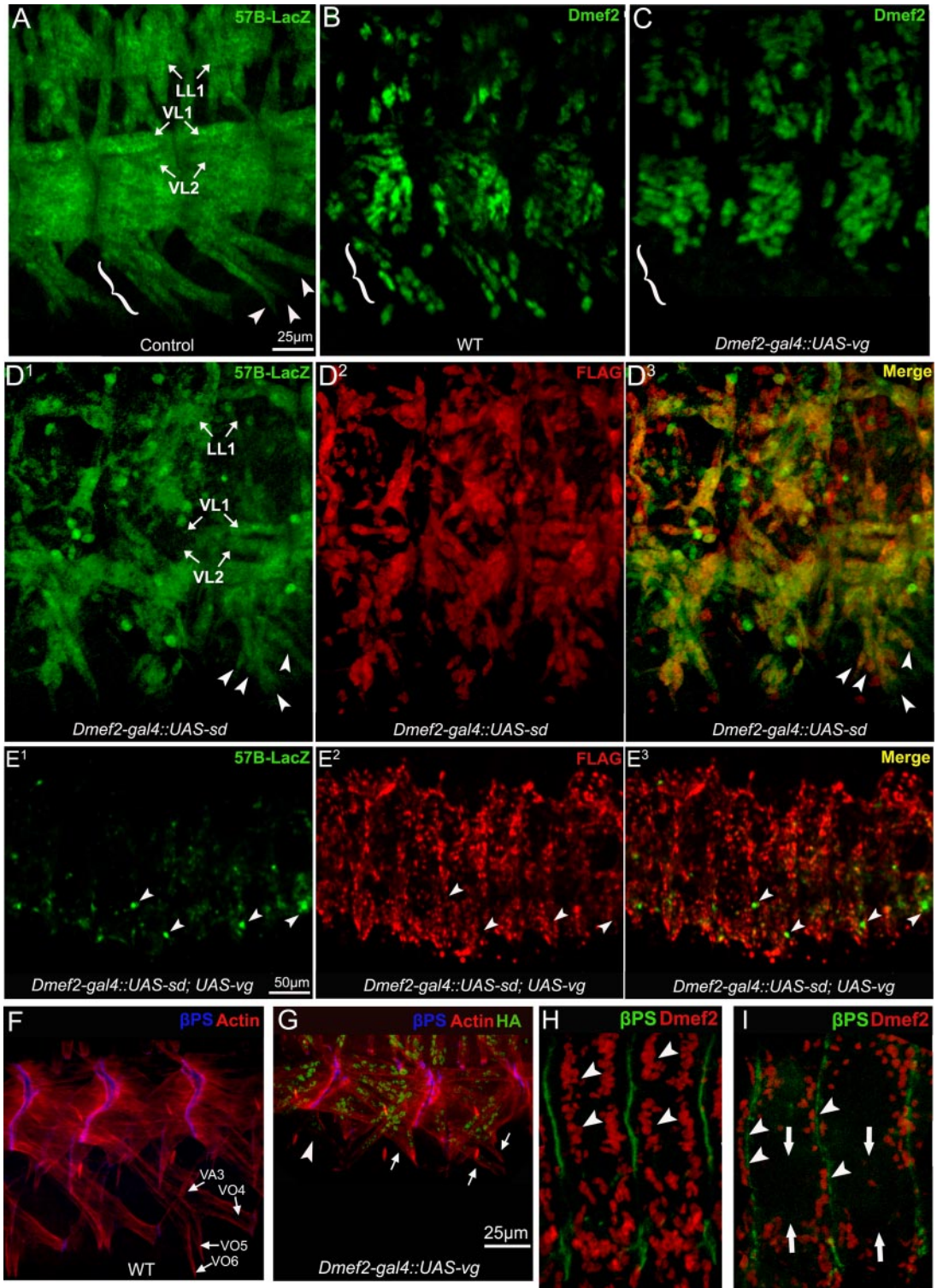

Figure 7. Ectopic-expression of Sd and/or Vg via *Dmef2*-GAL4 leads to abnormal development of somatic muscles. Embryos (stage 16) are shown as lateral views, and dorsal is up, with anterior to the left. (A) Muscle fibers are visualized by anti-β-Gal (green) in control embryos expressing LacZ in cytoplasm under the control of the *act57B* promoter shown in A. Arrows point to muscle LL1, VL1, and VL2, and the bracket shows the ventral oblique muscles (VO4-6, see Figure 3D). VO4-6 muscles produce three projections that expand posterior-ventrally. (B) Muscle cells are marked with anti-Dmef2 (green) in wild-type embryos. Bracket shows muscle VO4-6. (C) In embryos ectopically expressing 3xHA-Vg, the extension of VO4-6 is lost (arrows), but the DMs are still highly organized (compare B with C). (D^1–D^3) Embryos (*act57B-lacZ*) ectopically expressing 3xFLAG-Sd (red) have disorganized somatic muscles. LacZ

genes in a single muscle using a Gal4 driver specific for VL1 (Figure 6K). We see a corresponding reduction in actin or myosin expression in the VL1 muscle with increased expression of *sd* and *vg* (Figure 6, J and K). These reductions lead to the missing of myofiber in SMs (Figure 6, H and K). Altogether, these data indicate that Sd and Vg repress Dmef2 function during muscle differentiation.

Altered Expression of Sd and/or Vg Leads to Abnormal SM Development

As increased expression of Vg and Sd leads to reduction of muscle-specific markers like *act57B* and *mhc*, we next examined the fate of these cells (Figure 7). Because the mammalian homologues of Sd, Vg and Dmef2 have a role in terminal muscle differentiation (Chen *et al.*, 1994; Lilly *et al.*, 1995; Maeda *et al.*, 2002a), we used *Dmef2*-GAL4 to express transgene(s) in all mesodermal cells of late stage 7 embryos and later in cardiac cells of the heart, visceral, and somatic muscle cells until the end of embryogenesis (Ranganayakulu *et al.*, 1998). The pattern of the muscle system in wild-type embryos is shown in Figure 7, A and B. An *act57B*-LacZ transgene was used to visualize muscle fibers (Figure 7A) and to monitor for gross alterations in the expression level of *act57B* in muscle cells.

Expressing additional Vg in the somatic muscles seems to cause a complete loss of the VO4-6 muscles although the overall organization of the remaining muscles appears normal (Figure 7C). However, in embryos expressing UAS-*3xFLAG-sd*, the normal precise organization of muscle fibers is lost (Figure 7D and Supplemental Figure S2C). Specifically, we repeatedly see that muscle LL1 does not develop well or get lost and that muscle VL1-2 often disappear in many segments (Figure 7D). Unlike what is seen with ectopic Vg, the ventral muscle VO4-6 is still present but ectopic Sd expression seems to cause defects in migration with more projections than what is seen in wild type (Figure 7, A and D and Supplemental Figure S2C). Coexpression of UAS-*3xFLAG-sd* and UAS-*3xHA-vg* together in SMs causes repression of *act57B* in most cells (Figure 7E). In these embryos, the organization of muscle fibers is completely disrupted (Figure 7E and Supplemental Figure S2D). Actin staining of these embryos failed to visualize the muscle fibers, probably because there is little myofibril formation (Figure 6H). Expression of UAS-*3xFLAG-sd* in the *Dmef2* RNAi background produced similar phenotype to that of coexpression of UAS-*3xFLAG-sd* and UAS-*3xHA-vg* (Supplemental Figure S2E), further conforming that Sd and Vg repress Dmef2 function during muscle differentiation.

We further examined the organization of the developing muscles by staining for βPS-integrin, one of the major integrins, acting as a transmembrane protein that stabilizes attachments between two neighbor muscles and that between muscles and epidermis along the segment border (Volk and VijayRaghavan, 1994; Brown *et al.*, 2000). In wild-type embryos, muscle cells attach at characteristic positions relative to segment borders (Figure 7H). However, in embryos expressing UAS-*3xFLAG-sd* and UAS-*3xHA-vg*, the organization of muscle cell attachment is severely disrupted (Figure 7I). Embryos ectopically expressing UAS-*3xHA-vg* in SMs exhibit a different phenotype. SMs still have a highly organized pattern (Figure 7C), and muscle cells do not lose their positions (data not shown), but the migration of VO4-6 muscles seem to be inhibited or redirected (Figure 7, F and G). However, expression of UAS-*vg 3-9*, the Vg deletion that loses interaction with Dmef2 (Figure 5C), produced wild-type phenotype (data not shown). As a control, we examined embryos overexpressing UAS-*6xMyc-Dmef2,* and this does not cause any obvious defect in SMs (data not shown).

Altered Expression of Sd, Vg, and Dmef2 Causes Defects in Cardiac Cell Development

In wild-type, there is a single row of Dmef2-positive cardiac cells on each side of the embryo (Figure 8A) and four Tin-positive cardiac cells per hemisegment with some Tin-positive pericardial cells (Figure 8B, see Figure 2F for a diagram of each cardiac cell fate). It was reported previously that the *Dmef2*-GAL4 driver was not active in pericardial cells (Ranganayakulu *et al.*, 1998), but, based on our analysis of the pattern of *β-gal* expression driven by *Dmef2*-GAL4, it also drives expression, at least transiently, in pericardial cells (Figure 8A′). We used this driver for examining the effect of elevated levels of Vg or Sd on cardiac cell differentiation.

Ectopic expression of UAS-*3xHA-vg* does not affect the Dmef2-positive cardiac cells (Figure 8C), but causes two additional Tin-positive cardiac cells per hemisegment (Figure 8D). *Dmef2*-GAL4 induced expression of UAS-*3xFLAG-sd* causes two extra rows of Dmef2-positive cardiac cells (Figure 8E), whereas the total number of Tin-positive heart cells is similar to wild type (Figure 8F). However, this pattern of the differentiating cardiac cells becomes disorganized with some Tin-positive cells in the SM region (Figure 8F). Elevating the levels of Dmef2 using a UAS-*6xMyc-Dmef2* combination produces one extra row of Dmef2-positive cardiac cells (Figure 8G), but does not affect the Tin-positive cardiac cells (Figure 8H). Ectopic expression of UAS-*3xHA-vg* and UAS-*6xMyc-Dmef2* together has a synergistic effect, as there are two extra rows of Dmef2-positive cardiac cells (Figure 8I) and six Tin-positive cardiac cells per hemisegment with many more Tin-positive pericardial cells around (Figure 8J). Expression of UAS-*3xFLAG-sd* and UAS-*6xMyc-Dmef2* together causes a phenotype similar to that of embryos expressing UAS-*3xFLAG-sd* alone (Figure 8K-M). However, the pattern of heart cells is more organized (Figure 8M, compared with F), indicating a partial rescue of the phenotype. Expression of UAS-*3xFLAG-sd* and UAS-*3xHA-vg* together leads to loss of almost all Dmef2-positive cardiac cells (Figure 8N) and dislocation of all Tin-positive

Figure 7 (cont). staining shows the whole muscle and FLAG staining shows the muscle nuclei. Muscle LL1, VL1, and VL2 do not develop well or disappear in some segments (arrows). The ventral muscle VO4-6 can still produce projections that expand ventrally, but there are more projections than wild type, and some projections expand anterior-ventrally (arrowheads, compare D^1 with A). (E^1–E^3) Embryos (*act57B-lacZ*) ectopically expressing both 3xFLAG-Sd (red) and 3xHA-Vg have disorganized SMs, and the extension of VO4-6 is also lost (arrows). The expression level of LacZ is generally very low compared with the control, and cells with high expression levels usually do not express 3xFLAG-Sd or have low expression (arrowheads). Staining of 3xHA-Vg is not shown, because 3xFLAG-Sd and 3xHA-Vg always appear in the same muscle cells. (F) Wild-type ventral SMs (arrows) are labeled by phalloidin, and the segment border is labeled with anti-βPS-integrin. Arrows point to muscle VO4-6 and VA3. (G) In embryos overexpressing 3xHA-Vg, VL1-4 muscles are not affected, but ventral SMs are severely affected. It seems that these muscles are still there, but their migrations are either inhibited (arrowhead) or directed in a different path (arrows), which lead to no long extensions of muscle fiber. HA staining (green) shows the nuclei of muscles. (H) Wild-type SMs are labeled with anti-Dmef2 (red), and the segment border is labeled with anti-βPS-integrin. All muscle cells have their proper positions relative to the border (arrowheads). (I) In embryos overexpressing both 3xFLAG-Sd and 3xHA-Vg, muscle cells lose their positions and appear to cluster along the segments border (arrowheads). Large gaps are seen within each segment (arrows).

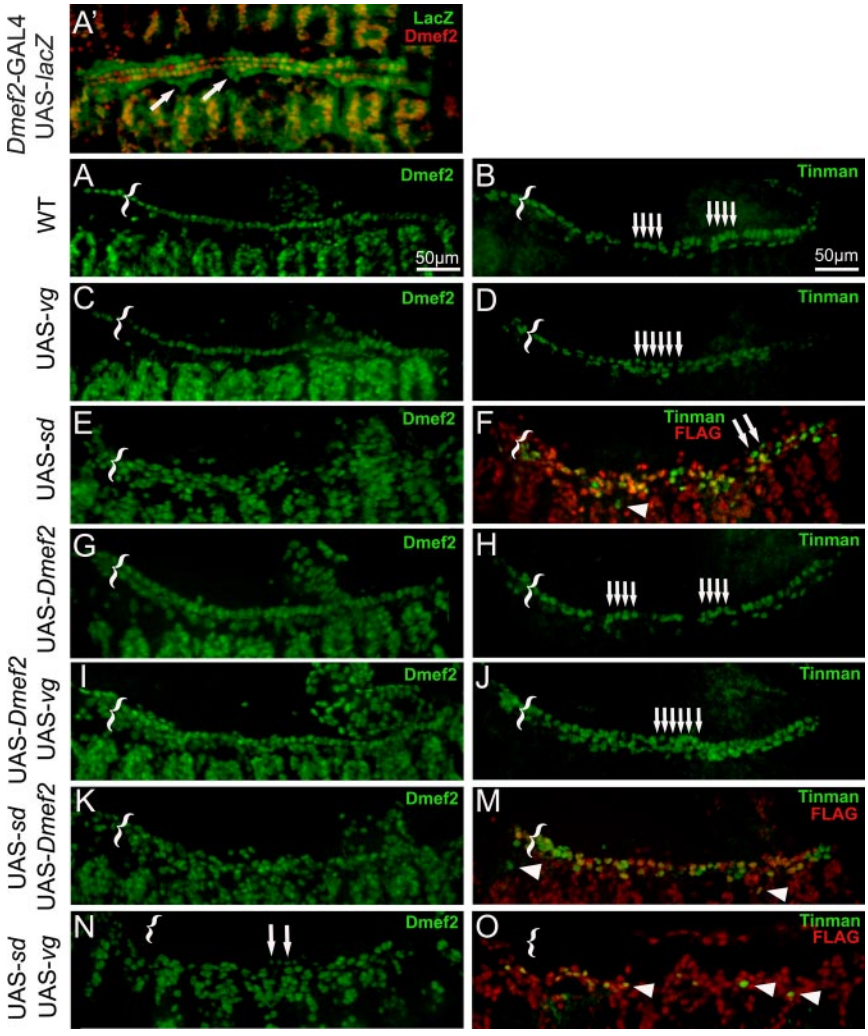

Figure 8. Functional interactions between Sd, Vg, and Dmef2 can be shown by ectopic expression of various combinations of Sd, Vg, and Dmef2 in heart cells. Embryos shown as lateral views and dorsal up with anterior to the left are at stage 14 and stained with antibodies as indicated by the colored lettering. Brackets show the area where the heart cells are located. (A′) *Dmef2*-GAL4 drives the expression of LacZ in all SMs and in both cardiac cells and pericardial cells (arrows). (A and B) Wild type. There is one row of Dmef2-positive cardiac cells (A) and four Tin-positive cardiac cells per hemisegment (B, arrows). (C and D) Embryos ectopic-expressing 3xHA-Vg have the normal one row of Dmef2-positive cardiac cells (C), but now have six Tin-positive cardiac cells per hemisegment (D, arrows). (E and F) Embryos ectopic-expressing 3xFLAG-Sd have two to three rows of Dmef2-positive cardiac cells (E). Tin-positive heart cells become disorganized: sometimes, you see only two Tin-positive cardiac cells in one hemisegment (F, arrows) and sometimes, you see Tin-positive cells appear in the region of the SMs (F, arrowhead). (G and H) Embryos overexpressing 6xMyc-Dmef2 have two rows of Dmef2-positive cardiac cells (G), but there are four Tin-positive cardiac cells per hemisegment like wild type (H, arrows). (I and J) Embryos overexpressing both 6xMyc-Dmef2 and 3xHA-Vg have two to three rows of Dmef2-positive cardiac cells (I) and six Tin-positive cardiac cells per hemisegment (J, arrows). Many more Tin-positive heart cells also appear (compared J with D and H). (K–M) Embryos overexpressing both 3xFLAG-Sd and 6xMyc-Dmef2. The phenotype is similar to E and F, but heart cells are more organized (compare M with F). Arrowheads show the Tin-positive cells mixed with SMs. (N and O) Embryos overexpressing both 3xFLAG-Sd and 3xHA-Vg have only a few Dmef2-positive cardiac cells left (N, arrows) and all the Tin-positive cells appear in the region of SMs (O, arrowheads).

cells in the SM region (Figure 8O). Finally, expression of the three transgenes together causes the same phenotype as that of expression of UAS-*3xFLAG-sd* and UAS-*3xHA-vg* together (data not shown). With the exception of embryos expressing UAS-*6xMyc-Dmef2*, all embryos died at the end of embryogenesis.

DISCUSSION

We have shown that there is an analogous requirement for the TEF-1 homologue, Sd, in the late-stage specification or differentiation of muscle cells. The cardiac phenotype associated with the sd^{3L} mutation (Figure 3) confirms that like mammalian TEF-1, there is a clear role for Sd in cardiac muscle differentiation. Expression of *sd* seems to be driven by the same elements that induce elevated *sd* expression in other tissues like the wing, because both the sd^{ETX4} and *Sd*-GAL4 reporters which were previously shown to faithfully report *sd* expression in wing imaginal discs, indirect flight muscles, and nervous system (Campbell *et al.*, 1992; Shyamala and Chopra, 1999) match the Sd expression pattern in embryonic muscles revealed by *sd* in situ (Figure 1). We have also determined that Vg, the first known TEF-1 family cofactor, has a role in SMs but not cardiac muscles (Figure 3H), and in fact, elevating Vg expression in the developing dorsal vessel has a negative effect on differentiation of this organ.

Our results show several lines of evidence supporting a model whereby Sd and Vg, in a complex with Dmef2, help to regulate late-stage *Drosophila* embryonic muscle development. One prediction of this model is that altering the relative levels of these proteins will have significant effects on specific subsets of muscle cells. The effect of the relative levels of each of these proteins can be observed in various cell types: 1) Sd and Dmef2 are coexpressed in the cardiac cells (Figure 2, A and B), where vg is not expressed; 2) Starting at stage 11, vg and Dmef2 are coexpressed in the progenitors of some SMs (Figure 2, C–E), where *sd* is expressed at a later stage (Figure 2, C–E); and 3) These three genes are coexpressed in SMs, DA1-3, LL-1, and VL1-4 at early stage 16 (Figure 2D), but by late stage 16 the coexpression is restricted to some ventral SMs (Figure 2E). We have also shown that 1) Sd is able to interact with Dmef2 without the presence of Vg (Figure 4, B and C); 2) Vg is able to interact with Dmef2 without the presence of Sd (Figure 4D); and 3) It is also possible for Sd, Vg and Dmef2 to form a tripartite complex (Figure 4A). Given that Vg appears to bind Dmef2 at two different sites, it may be that Vg could be the bridge protein connecting Sd and Dmef2, because Vg can bind each of them via a different domain (Figure 5, B and C).

Finally, a requirement for the presence of Sd and Vg appears to be specific to differentiation of specific muscle types as mutations in *sd* and *vg* cause defects in different muscles (Figure 3), whereas alterations in the relative expression levels of any of these three genes in developing muscles of *Drosophila* caused specific alterations in both SM and cardiomyoctes (Figures 7 and 8).

Because our data show that Vg can bind Dmef2 independently of Sd, it is possible that Vg may modify Dmef2 activity in the absence of Sd. We noted that the *vg* and *Dmef2* genes are coexpressed in some SMs (DA1-3, LL1, and VL1-4) before Sd is present in those muscles (Figure 2, C–E). They are also coexpressed in the progenitors of muscle VL1-4. We also show that functional interactions exist between Vg and Dmef2, as coexpression of them in heart cells has a synergistic effect on increasing the numbers of Dmef2-positive and Tin-positive cardiac cells (Figure 8, I and J), and the phenotype of vg^{null} mutant is enhanced in a *Dmef2* deficiency background (Supplemental Figure S2F). Previous studies of *vg* have almost exclusively focused on its function as a wing identity gene. However, there is now mounting evidence that Vg also defines the cellular identity of a subgroup of embryonic SMs (Figures 3 and 7, C and G; Baylies *et al.*, 1998; Sudarsan *et al.*, 2001), although the functional role of Vg in the development of these muscles is not clear. *Dmef2* is considered to be a "differentiation gene" playing a role in the final stages of muscle differentiation. Thus, this begs the question: what is the significance of the interaction between these two proteins that apparently have roles at different developmental stages? A recent study showed that Dmef2 not only binds to regulatory regions of muscle structural genes but also binds many muscle "identity genes" and genes involved in early signal pathways of muscle development (Sandmann *et al.*, 2006), indicating a role of *Dmef2* in early muscle development. Therefore, Vg may act together with Dmef2 to specify those SMs in which Vg is expressed. Our data support this idea, because vg^{null} mutants often lose muscle V_L-2 (Figure 3H), and overexpression of Sd leads to either poor development or loss of muscle LL1 and VL1-4 (Figure 7, D^1–D^3) where Vg is present. Considering the strong functional interaction that is known to occur between Vg and Sd (Simmonds *et al.*, 1998), overexpression of Sd may interfere with the function of Vg in those muscles.

Just as Vg and Dmef2 may interact in the absence of Sd, a Sd/Dmef2 complex may exist in muscle cells where *vg* is not expressed significantly; i.e., cardiac cells in the heart region and some somatic muscle cells (Figure 2). Expression of UAS-*6Myc-Dmef2* via *Dmef2*-GAL4 results in one extra row of Dmef2-positive cardiac cells (Figure 8G). This phenotype is not unexpected as *Dmef2*-GAL4 is also active in pericardial cells that surround cardiac cells (Figure 8A′). However, it is unexpected that expression of UAS-*3xFlAG-sd* also produces extra rows of Dmef2-positive cardiac cells (Figure 8E). These results indicate that Sd could activate the expression of Dmef2 in the pericardial cells. Because the pattern of expression directed by the enhancer of *Dmef2* in muscle cells is very complicated (Nguyen and Xu, 1998) it has been proposed that there is an autoregulation mechanism to maintain its expression in differentiated muscles (Cripps *et al.*, 2004). Therefore, Sd might be required to act with Dmef2 to maintain expression of Dmef2 in cardiac cells at late stages. The ability of Dmef2 to partially rescue the heart phenotype caused by expression of UAS-*3xFLAG-sd* (Figure 8, K–M) also suggests a functional interaction between Sd and Dmef2, because Sd itself does not have transcriptional activation ability and overexpression of Sd can lead to repression of transcription (Simmonds *et al.*, 1998).

Mutation and ectopic-expression analysis also revealed that Sd has a role in both heart muscle and SM development (Figure 3). Recently, Sd was shown to be the target of the Hippo (Hpo) signaling pathway that governs cell growth, proliferation, and apoptosis (Zhang *et al.*, 2008). Inactivation of Sd diminishes Hpo target gene expression and reduces organ size, whereas a constitutively active Sd promotes tissue overgrowth (Zhang *et al.*, 2008). We see that in sd^{3L} mutants there are fewer heart cells and that the VO4-6 muscles appear to have defects in their differentiation (Figure 3, A–F), whereas overexpression of Sd in VO4-6 produces more projections (Figure 7D). These phenotypes would suggest a role of Sd in both growth and proliferation of muscle cells. Conversely, ectopic expression of Vg in VO4-6 muscles leads to a phenotype similar to that of sd^{3L} (Figure 7, F and G). Thus, it appears that ectopic expression of Vg in those muscles interferes with the function of Sd.

We observed that coexpression of UAS-*3xFLAG-sd* and UAS-*3xHA-vg* for extended times via *Dmef2*-GAL4 causes significant defects in muscle differentiation, including significant alterations in their sites of attachment. In cardiac muscles, Tin-positive heart cells end up in the SM region (Figure 8O); by the end of muscle development, the stereotyped patterning of SMs is totally disrupted (Figure 7E). This phenotype may be a result of the apparent dynamic expression we observe of the *sd* reporters in SMs (Figure 2). Thus, any Sd–Vg complex that would be formed in developing muscles would be transient, freeing each potential cofactor to interact with Dmef2 independently.

It is interesting that Sd–Vg complex represses Dmef2 function without affecting Dmef2 expression during muscle development (Figure 6 and Supplemental Figure S2E). The protein Him (Holes in muscle) was also shown before to repress Dmef2 function during muscle differentiation, and the authors argue that a balance of positive and negative inputs controls muscle differentiation (Liotta *et al.*, 2007). Our data support this idea and may reveal another layer of negative input, the Sd–Vg complex, in muscle differentiation, because overexpression of Sd or Sd and Vg produces a phenotype similar to that of overexpression of Him in developing SMs (Figure 6, E and F) and also to that of *Dmef2* RNAi embryos. The repression we see of *act57B*, the product of which is primarily required during muscle differentiation, may be a normal occurrence during late stage 16 when most SMs are presumably fully differentiated, having finished migration and reached their attachment sites (Schnorrer and Dickson, 2004). At this time, some SMs in different segments contact each other and specific extracellular matrix (ECM) contacts between muscles form (Martin-Bermudo, 2000; Martin-Bermudo and Brown, 2000). *act57B* is initially expressed in SMs at stage11, and by stage16 there is already high levels of *act57B* transcript in SMs (Kelly *et al.*, 2002). Specifically, these SMs would slow myofibril growth by repressing the expression of *act57B*, especially in those SMs that contact with neighboring muscles, like LL1 and VL1-4, and the presence of Vg in these muscles (Figure 3H) may be mediating this repression.

The most significant repression of Dmef2 function appears to require the presence of both Sd and Vg (Figure 6F and Supplemental Figure S2D). However, this is at odds with the presumptive activating function mediated by an Sd–Vg complex that occurs in other tissues like the wing imaginal disk, where an Sd–Vg complex binds and activates the *vg* boundary enhancer (Halder *et al.*, 1998). The differential activities of these proteins in muscle versus wing development may reflect a requirement for yet additional proteins within a presumptive Vg/Sd/Dmef2 complex to modify its

activity in a tissue-specific manner. Alternatively, posttranslational modifications to Vg or Sd (or both) may modify their activity. Interestingly, the yeast Sd homologue, Tec1, is phosphorylated and then degraded during the mating pheromone response (Bao *et al.*, 2004). In mammals, TEF-1 is phosphorylated responding to cAMP/PK-A signaling (Gupta *et al.*, 2000). However, there is, as yet, no clear indication that Sd is phosphorylated in *Drosophila* cells.

Finally, although we have shown that Sd, Vg, and Dmef2 interact directly, similar to their mammalian homologues, our data suggest potential new functions of Sd and Vg during muscle specification. For example, Vg seems to have role in the specification of ventral muscles VL1-4, and Sd has a role in the development of muscle VO4-6, especially in the development of their projections. In addition, the Sd–Vg complex represses Dmef2 function, which is at odds with the known activities of their mammalian homologues. However, this repression only happens in certain muscles (e.g., VL1-4) that need to contact neighboring muscles.

ACKNOWLEDGMENTS

We thank B. Paterson for the Dmef2 antibody and Richard M. Cripps (University of New Mexico, Albuquerque, NM) for the *actin57B* construct. We thank Shelagh Campbell and members of the Simmonds lab for reading and commenting on the manuscript. A.J.S. is an Alberta Heritage Foundation for Medical Research Senior Scholar. This research was supported by a Grant-in-aid from the Heart and Stroke Foundation of Alberta, Northwest Territories and Nunavut to A.J.S. and J.B. and a National Sciences and Engineering Research Council Discovery Grant to J.B.

REFERENCES

Azpiazu, N., and Frasch, M. (1993). tinman and bagpipe: two homeo box genes that determine cell fates in the dorsal mesoderm of *Drosophila.* Genes Dev. *7*, 1325–1340.

Bao, M. Z., Schwartz, M. A., Cantin, G. T., Yates, J. R., 3rd, and Madhani, H. D. (2004). Pheromone-dependent destruction of the Tec1 transcription factor is required for MAP kinase signaling specificity in yeast. Cell *119*, 991–1000.

Bate, M., and Rushton, E. (1993). Myogenesis and muscle patterning in *Drosophila.* C. R. Acad. Sci. III *316*, 1047–1061.

Baylies, M. K., Bate, M., and Ruiz Gomez, M. (1998). Myogenesis: a view from *Drosophila.* Cell *93*, 921–927.

Bernard, F., Lalouette, A., Gullaud, M., Jeantet, A. Y., Cossard, R., Zider, A., Ferveur, J. F., and Silber, J. (2003). Control of apterous by vestigial drives indirect flight muscle development in *Drosophila.* Dev. Biol. *260*, 391–403.

Black, B. L., Molkentin, J. D., and Olson, E. N. (1998). Multiple roles for the MyoD basic region in transmission of transcriptional activation signals and interaction with MEF2. Mol. Cell Biol. *18*, 69–77.

Black, B. L., and Olson, E. N. (1998). Transcriptional control of muscle development by myocyte enhancer factor-2 (MEF2) proteins. Annu. Rev. Cell Dev. Biol. *14*, 167–196.

Brand, A. H., and Perrimon, N. (1993). Targeted gene expression as a means of altering cell fates and generating dominant phenotypes. Development *118*, 401–415.

Brown, N. H., Gregory, S. L., and Martin-Bermudo, M. D. (2000). Integrins as mediators of morphogenesis in *Drosophila.* Dev. Biol. *223*, 1–16.

Butler, A. J., and Ordahl, C. P. (1999). Poly(ADP-ribose) polymerase binds with transcription enhancer factor 1 to MCAT1 elements to regulate muscle-specific transcription. Mol. Cell Biol. *19*, 296–306.

Campbell, S., Inamdar, M., Rodrigues, V., Raghavan, V., Palazzolo, M., and Chovnick, A. (1992). The scalloped gene encodes a novel, evolutionarily conserved transcription factor required for sensory organ differentiation in *Drosophila.* Genes Dev. *6*, 367–379.

Campbell, S. D., Duttaroy, A., Katzen, A. L., and Chovnick, A. (1991). Cloning and characterization of the scalloped region of *Drosophila melanogaster*. Genetics *127*, 367–380.

Carlini, L. E., Getz, M. J., Strauch, A. R., and Kelm, R. J., Jr. (2002). Cryptic MCAT enhancer regulation in fibroblasts and smooth muscle cells. Suppression of TEF-1 mediated activation by the single-stranded DNA-binding proteins, Pur alpha, Pur beta, and MSY1. J. Biol. Chem. *277*, 8682–8692.

Charron, F., and Nemer, M. (1999). GATA transcription factors and cardiac development. Semin. Cell Dev. Biol. *10*, 85–91.

Chen, H. H., Mullett, S. J., and Stewart, A. F. (2004). Vgl-4, a novel member of the vestigial-like family of transcription cofactors, regulates alpha1-adrenergic activation of gene expression in cardiac myocytes. J. Biol. Chem. *279*, 30800–30806.

Chen, Z., Friedrich, G. A., and Soriano, P. (1994). Transcriptional enhancer factor 1 disruption by a retroviral gene trap leads to heart defects and embryonic lethality in mice. Genes Dev. *8*, 2293–2301.

Cripps, R. M., Lovato, T. L., and Olson, E. N. (2004). Positive autoregulation of the Myocyte enhancer factor-2 myogenic control gene during somatic muscle development in *Drosophila.* Dev. Biol. *267*, 536–547.

Cripps, R. M., and Olson, E. N. (2002). Control of cardiac development by an evolutionarily conserved transcriptional network. Dev. Biol. *246*, 14–28.

Crossley, A. C. (1978). The morphology of the *Drosophila* muscular system. In: The Genetics and Biology of *Drosophila*, Vol. 2b, ed. M. Ashburner and T. Wright, New York: Academic Press, 499–560.

Deshpande, N., Chopra, A., Rangarajan, A., Shashidhara, L. S., Rodrigues, V., and Krishna, S. (1997). The human transcription enhancer factor-1, TEF-1, can substitute for *Drosophila* scalloped during wingblade development. J. Biol. Chem. *272*, 10664–10668.

Gajewski, K., Kim, Y., Lee, Y. M., Olson, E. N., and Schulz, R. A. (1997). D-mef2 is a target for Tinman activation during *Drosophila* heart development. EMBO J. *16*, 515–522.

Gunther, S., Mielcarek, M., Kruger, M., and Braun, T. (2004). VITO-1 is an essential cofactor of TEF1-dependent muscle-specific gene regulation. Nucleic Acids Res. *32*, 791–802.

Gupta, M., Kogut, P., Davis, F. J., Belaguli, N. S., Schwartz, R. J., and Gupta, M. P. (2001). Physical interaction between the MADS box of serum response factor and the TEA/ATTS DNA-binding domain of transcription enhancer factor-1. J. Biol. Chem. *276*, 10413–10422.

Gupta, M. P., Amin, C. S., Gupta, M., Hay, N., and Zak, R. (1997). Transcription enhancer factor 1 interacts with a basic helix-loop-helix zipper protein, Max, for positive regulation of cardiac alpha-myosin heavy-chain gene expression. Mol. Cell. Biol. *17*, 3924–3936.

Gupta, M. P., Kogut, P., and Gupta, M. (2000). Protein kinase-A dependent phosphorylation of transcription enhancer factor-1 represses its DNA-binding activity but enhances its gene activation ability. Nucleic Acids Res. *28*, 3168–3177.

Halder, G., Polaczyk, P., Kraus, M. E., Hudson, A., Kim, J., Laughon, A., and Carroll, S. (1998). The Vestigial and Scalloped proteins act together to directly regulate wing-specific gene expression in *Drosophila*. Genes Dev. *12*, 3900–3909.

Han, K. (1996). An efficient DDAB-mediated transfection of *Drosophila* S2 cells. Nucleic Acids Res. *24*, 4362–4363.

Han, Z., Yi, P., Li, X., and Olson, E. N. (2006). Hand, an evolutionarily conserved bHLH transcription factor required for *Drosophila* cardiogenesis and hematopoiesis. Development *133*, 1175–1182.

Hughes, S. C., and Krause, H. M. (1999). Single and double FISH protocols for *Drosophila.* Methods Mol. Biol. *122*, 93–101.

Jiang, S. W., and Eberhardt, N. L. (1996). TEF-1 transrepression in BeWo cells is mediated through interactions with the TATA-binding protein, TBP. J. Biol. Chem. *271*, 9510–9518.

Kaelin, W. G., Jr., Pallas, D. C., DeCaprio, J. A., Kaye, F. J., and Livingston, D. M. (1991). Identification of cellular proteins that can interact specifically with the T/E1A-binding region of the retinoblastoma gene product. Cell *64*, 521–532.

Kelly, K. K., Meadows, S. M., and Cripps, R. M. (2002). *Drosophila* MEF2 is a direct regulator of Actin57B transcription in cardiac, skeletal, and visceral muscle lineages. Mech. Dev. *110*, 39–50.

Lecuyer, E., Yoshida, H., Parthasarathy, N., Alm, C., Babak, T., Cerovina, T., Hughes, T. R., Tomancak, P., and Krause, H. M. (2007). Global analysis of mRNA localization reveals a prominent role in organizing cellular architecture and function. Cell *131*, 174–187.

Lilly, B., Galewsky, S., Firulli, A. B., Schulz, R. A., and Olson, E. N. (1994). D-MEF2, a MADS box transcription factor expressed in differentiating mesoderm and muscle cell lineages during *Drosophila* embryogenesis. Proc. Natl. Acad. Sci. USA *91*, 5662–5666.

Lilly, B., Zhao, B., Ranganayakulu, G., Paterson, B. M., Schulz, R. A., and Olson, E. N. (1995). Requirement of MADS domain transcription factor D-MEF2 for muscle formation in *Drosophila.* Science *267*, 688–693.

Lin, M. H., Nguyen, H. T., Dybala, C., and Storti, R. V. (1996). Myocyte-specific enhancer factor 2 acts cooperatively with a muscle activator region to regulate *Drosophila* tropomyosin gene muscle expression. Proc. Natl. Acad. Sci. USA *93*, 4623–4628.

Liotta, D., Han, J., Elgar, S., Garvey, C., Han, Z., and Taylor, M. V. (2007). The Him gene reveals a balance of inputs controlling muscle differentiation in *Drosophila*. Curr. Biol. *17*, 1409–1413.

MacKay, J. O., Soanes, K. H., Srivastava, A., Simmonds, A., Brook, W. J., and Bell, J. B. (2003). An in vivo analysis of the vestigial gene in *Drosophila melanogaster* defines the domains required for Vg function. Genetics *163*, 1365–1373.

Maeda, T., Chapman, D. L., and Stewart, A. F. (2002a). Mammalian vestigial-like 2, a cofactor of TEF-1 and MEF2 transcription factors that promotes skeletal muscle differentiation. J. Biol. Chem. *277*, 48889–48898.

Maeda, T., Gupta, M. P., and Stewart, A. F. (2002b). TEF-1 and MEF2 transcription factors interact to regulate muscle-specific promoters. Biochem. Biophys. Res. Commun. *294*, 791–797.

Martin-Bermudo, M. D. (2000). Integrins modulate the Egfr signaling pathway to regulate tendon cell differentiation in the *Drosophila* embryo. Development *127*, 2607–2615.

Martin-Bermudo, M. D., and Brown, N. H. (2000). The localized assembly of extracellular matrix integrin ligands requires cell-cell contact. J. Cell Sci. *113*(Pt 21), 3715–3723.

Mas, J. A., Garcia-Zaragoza, E., and Cervera, M. (2004). Two functionally identical modular enhancers in *Drosophila* troponin T gene establish the correct protein levels in different muscle types. Mol. Biol. Cell *15*, 1931–1945.

Molkentin, J. D., Black, B. L., Martin, J. F., and Olson, E. N. (1995). Cooperative activation of muscle gene expression by MEF2 and myogenic bHLH proteins. Cell *83*, 1125–1136.

Morin, S., Charron, F., Robitaille, L., and Nemer, M. (2000). GATA-dependent recruitment of MEF2 proteins to target promoters. EMBO J. *19*, 2046–2055.

Morin, S., Pozzulo, G., Robitaille, L., Cross, J., and Nemer, M. (2005). MEF2-dependent recruitment of the HAND1 transcription factor results in synergistic activation of target promoters. J. Biol. Chem. *280*, 32272–32278.

Muller, D., Kugler, S. J., Preiss, A., Maier, D., and Nagel, A. C. (2005). Genetic modifier screens on Hairless gain-of-function phenotypes reveal genes involved in cell differentiation, cell growth and apoptosis in *Drosophila melanogaster*. Genetics *171*, 1137–1152.

Nguyen, H. T., and Xu, X. (1998). Drosophila mef2 expression during mesoderm development is controlled by a complex array of cis-acting regulatory modules. Dev. Biol. *204*, 550–566.

Nguyen, T., Wang, J., and Schulz, R. A. (2002). Mutations within the conserved MADS box of the D-MEF2 muscle differentiation factor result in a loss of DNA binding ability and lethality in *Drosophila*. Differentiation *70*, 438–446.

Nongthomba, U., Clark, S., Cummins, M., Ansari, M., Stark, M., and Sparrow, J. C. (2004). Troponin I is required for myofibrillogenesis and sarcomere formation in *Drosophila* flight muscle. J. Cell Sci. *117*, 1795–1805.

Pasquet, S., Naye, F., Faucheux, C., Bronchain, O., Chesneau, A., Thiebaud, P., and Theze, N. (2006). Transcription enhancer factor-1-dependent expression of the alpha-tropomyosin gene in the three muscle cell types. J. Biol. Chem. *281*, 34406–34420.

Ranganayakulu, G., Elliott, D. A., Harvey, R. P., and Olson, E. N. (1998). Divergent roles for NK-2 class homeobox genes in cardiogenesis in flies and mice. Development *125*, 3037–3048.

Ritzenthaler, S., Suzuki, E., and Chiba, A. (2000). Postsynaptic filopodia in muscle cells interact with innervating motoneuron axons. Nat. Neurosci. *3*, 1012–1017.

Roy, S., Shashidhara, L. S., and VijayRaghavan, K. (1997). Muscles in the *Drosophila* second thoracic segment are patterned independently of autonomous homeotic gene function. Curr. Biol. *7*, 222–227.

Sandmann, T., Jensen, L. J., Jakobsen, J. S., Karzynski, M. M., Eichenlaub, M. P., Bork, P., and Furlong, E. E. (2006). A temporal map of transcription factor activity: mef2 directly regulates target genes at all stages of muscle development. Dev. Cell *10*, 797–807.

Schnorrer, F., and Dickson, B. J. (2004). Muscle building; mechanisms of myotube guidance and attachment site selection. Dev. Cell *7*, 9–20.

Shyamala, B. V., and Chopra, A. (1999). *Drosophila melanogaster* chemosensory and muscle development: identification and properties of a novel allele of scalloped and of a new locus, SG18.1, in a Gal4 enhancer trap screen. J. Genet. *78*, 87–97.

Simmonds, A. J., Liu, X., Soanes, K. H., Krause, H. M., Irvine, K. D., and Bell, J. B. (1998). Molecular interactions between Vestigial and Scalloped promote wing formation in *Drosophila*. Genes Dev. *12*, 3815–3820.

Srivastava, A., MacKay, J. O., and Bell, J. B. (2002). A Vestigial:Scalloped TEA domain chimera rescues the wing phenotype of a scalloped mutation in *Drosophila melanogaster*. Genesis *33*, 40–47.

Srivastava, A., Simmonds, A. J., Garg, A., Fossheim, L., Campbell, S. D., and Bell, J. B. (2004). Molecular and functional analysis of scalloped recessive lethal alleles in *Drosophila melanogaster*. Genetics *166*, 1833–1843.

Stewart, A. F., Larkin, S. B., Farrance, I. K., Mar, J. H., Hall, D. E., and Ordahl, C. P. (1994). Muscle-enriched TEF-1 isoforms bind M-CAT elements from muscle-specific promoters and differentially activate transcription. J. Biol. Chem. *269*, 3147–3150.

Sudarsan, V., Anant, S., Guptan, P., VijayRaghavan, K., and Skaer, H. (2001). Myoblast diversification and ectodermal signaling in *Drosophila*. Dev. Cell *1*, 829–839.

Varadarajan, S., and VijayRaghavan, K. (1999). scalloped functions in a regulatory loop with vestigial and wingless to pattern the *Drosophila* wing. Dev. Genes Evol. *209*, 10–17.

Vassilev, A., Kaneko, K. J., Shu, H., Zhao, Y., and DePamphilis, M. L. (2001). TEAD/TEF transcription factors utilize the activation domain of YAP65, a Src/Yes-associated protein localized in the cytoplasm. Genes Dev. *15*, 1229–1241.

Vaudin, P., Delanoue, R., Davidson, I., Silber, J., and Zider, A. (1999). TONDU (TDU), a novel human protein related to the product of vestigial (vg) gene of *Drosophila melanogaster* interacts with vertebrate TEF factors and substitutes for Vg function in wing formation. Development *126*, 4807–4816.

Volk, T., and VijayRaghavan, K. (1994). A central role for epidermal segment border cells in the induction of muscle patterning in the *Drosophila* embryo. Development *120*, 59–70.

Xiao, J. H., Davidson, I., Matthes, H., Garnier, J. M., and Chambon, P. (1991). Cloning, expression, and transcriptional properties of the human enhancer factor TEF-1. Cell *65*, 551–568.

Zhang, L., Ren, F., Zhang, Q., Chen, Y., Wang, B., and Jiang, J. (2008). The TEAD/TEF family of transcription factor Scalloped mediates Hippo signaling in organ size control. Dev. Cell *14*, 377–387.